

# PdAu Based Resistive Hydrogen Sensor in Anaerobic Environment

Clément Occelli, Tomas Fiorido, Carine Perrin-Pellegrino, Jean-Luc Seguin

► **To cite this version:**

Clément Occelli, Tomas Fiorido, Carine Perrin-Pellegrino, Jean-Luc Seguin. PdAu Based Resistive Hydrogen Sensor in Anaerobic Environment. SENSORCOMM 2021, Nov 2021, Athen, Greece. hal-03428722

**HAL Id: hal-03428722**

**<https://hal-amu.archives-ouvertes.fr/hal-03428722>**

Submitted on 15 Nov 2021

**HAL** is a multi-disciplinary open access archive for the deposit and dissemination of scientific research documents, whether they are published or not. The documents may come from teaching and research institutions in France or abroad, or from public or private research centers.

L'archive ouverte pluridisciplinaire **HAL**, est destinée au dépôt et à la diffusion de documents scientifiques de niveau recherche, publiés ou non, émanant des établissements d'enseignement et de recherche français ou étrangers, des laboratoires publics ou privés.

# PdAu Based Resistive Hydrogen Sensor in Anaerobic Environment

Clément Occelli, Tomas Fiorido, Carine Perrin-Pellegrino, Jean-Luc Seguin

Aix-Marseille Univ, Univ Toulon, CNRS, IM2NP  
Marseille, 13397, France

e-mails : {clement.occelli, tomas.fiorido, carine.perrin-pellegrino and jean-luc.seguin}@im2np.fr

**Abstract**—Hydrogen is a promising gas for greenhouse gas emission reduction but also a reactive one. Thus, sensor for hydrogen detection in various atmospheres is mandatory. While leak sensors in air environments have been widely studied, only few researches have been done for hydrogen detection in anaerobic environments. In this work, the electrical resistance variation of a PdAu alloy as a sensitive film, is studied at various temperatures for hydrogen exposures in an anaerobic (N<sub>2</sub>) environment. The Pd<sub>0.8</sub>Au<sub>0.2</sub> alloy was deposited on a Si/SiO<sub>2</sub> substrate using magnetron sputtering followed by annealing at 200°C in N<sub>2</sub>. The sensor was then tested at various temperatures for 0.3% H<sub>2</sub> exposure, the best operating temperature was found to be 50°C. Finally, sensor was able to detect at 50°C, concentrations from 0.3 to 3% H<sub>2</sub>. These preliminary results are promising for further development of hydrogen sensors in anaerobic environment.

**Keywords**—Hydrogen; PdAu; Resistive sensor; Anaerobic.

## I. INTRODUCTION

The current context of climate change and the drive for sustainable development require the reduction of greenhouse gas emissions through the introduction of new technologies with minimal or no carbon emissions. Hydrogen gas has been identified as a very attractive energy carrier, since its combustion and its use to produce electricity generate only water as by-products [1]–[3]. As a result, a fast-growing hydrogen economy, based on the replacement of fossil fuels by hydrogen, will become a reality in several countries. Hydrogen is the lightest of chemical elements and the smallest molecule, having a great propensity to leak. Furthermore, hydrogen is a colourless, odourless, and tasteless gas, which has low auto ignition concentration in air (4 to 75%). Hence, high sensitivity hydrogen sensors, able to detect any leakage of hydrogen, are essentials wherever hydrogen is produced, transported and used. Gas pipelines are considered as a way to transport hydrogen (as a hydrogen/natural gas mixture) toward the end user, avoiding construction of new costly infrastructures and facilitate long term storage [4]–[6]. Gas impurities such as humidity and SO<sub>2</sub> are kept to a minimum limiting the corrosion and fragilization of pipelines [7] [8]. As a result, output gas can be considered as almost perfectly dry. While sensors for the detection of hydrogen leaks into the air have been widely studied for decades [9]–[11], no comprehensive study has yet been published on the measurement of high hydrogen concentrations in an oxygen-deprived atmosphere. To our knowledge, only two papers have focused on the anaerobic operation of hydrogen sensors [12] [13].

The main sensor technology able to measure selectively high hydrogen concentrations is Palladium (Pd) based thin film resistive sensors [10] [14]. Indeed, the Pd surface atoms decompose the adsorbed hydrogen molecules, and atomic hydrogen is easily absorbed into the Pd bulk to form Pd hydride. The absorbed hydrogen atoms cause changes in the

crystal structure of the metal and an increase of electrical resistivity due to scattering of free electrons by the absorbed hydrogen atoms. However, the absorption of hydrogen causes an expansion of the Pd crystal lattice, leading to hysteresis in the sensor response and crack formation and delamination from the substrate.

One solution to avoid these serious drawbacks is to introduce, into Pd, metal atoms with an atomic radius larger than that of Pd atoms, e.g., Gold (Au) atoms. Hence, Au atoms, which occupy Pd lattice sites, slightly expand the Pd lattice, thereby reducing the strain induced energy barrier created upon hydrogen absorption, and thus hysteresis. As a result, hysteresis shrinks symmetrically and disappears about 20-25 % Au at room temperature [15] [16].

PdAu alloys were mainly used to realize optical sensors showing interesting performances [15], [17]–[19], but optical sensors are more complex and expensive than resistive sensors.

In this paper, we present preliminary results on the fabrication, characterisation and dry anaerobic sensing properties of a Pd<sub>0.8</sub>Au<sub>0.2</sub> resistive hydrogen sensor. The paper is structured as follow: in section II we will describe the sensor fabrication and the experimental setup used for sensing characterization; then, in section III, the sensing results under various temperatures and hydrogen exposures will be discussed. Finally, in section IV, a conclusion is drawn with an insight of future work.

## II. DESCRIPTION OF APPROACH AND TECHNIQUES

### A. Sensor fabrication

PdAu deposition was made by radio frequency magnetron sputtering. Prior to the sensor fabrication, SiO<sub>2</sub>/Si substrates were cleaned in an ultrasonic acetone bath followed by an alcohol and deionized water rinsing. Two cleaned substrates were placed in the sputtering chamber: one for structural characterization (sample A), the other for sensor realization (sample B). To allow rapid characterisation of hydrogen sensing, a simple basic sensor was made using a shadow mask consisting of a thin sheet of steel mechanically drilled. A picture of a typical fabricated sensor is shown in Fig. 1. The chamber was first pumped to a vacuum of  $5 \times 10^{-9}$  bar, then a thin titanium layer was deposited to promote adherence to the substrate as reported by several authors [20] [21]. The sputtering was performed on a Pd target partially covered by Au disks, at an argon pressure of  $15 \times 10^{-6}$  bar. Once deposition completed, the samples were annealed at 200°C in N<sub>2</sub> gas for several hours, since 200°C was found to be the best annealing temperature as described in [22]. Finally, a 120nm thick film was obtained, measurements were performed using a Dektak XT profilometer.

### B. Experimental Setup for Sensor Characterization

The sensor was tested in a chamber of approximately 0.3 litre. Sensor was positioned on a heating plate with a Pt100

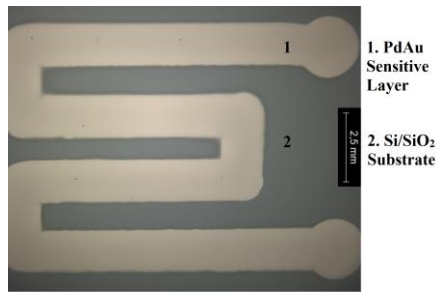


Figure 1. Optical microscope picture of a PdAu sensor made by sputtering.

(class B accuracy) temperature sensor attached next to it. The electrical resistance of the sensing film was measured by a Keithley Sourcemeeter 2450 and recorded on a personal computer by a homemade software, every 0.5s. A programmable commercial gas mixing system was used for flow regulation. A continuous dry nitrogen (N<sub>2</sub>) flow was used as baseline for every electrical measurement presented below. Hydrogen (H<sub>2</sub>) concentrations were obtained by mixing a 3% H<sub>2</sub> in N<sub>2</sub> bottle with a pure N<sub>2</sub> bottle (used for baseline). Every H<sub>2</sub> exposure last 25 min. A 100sccm gas flow at atmospheric pressure was used on every experiment. As electrical resistance varies with temperature, only the sensor response (R<sub>s</sub>) is calculated and presented in this work, using (1), where R<sub>0</sub> is the value of sensor stable base line resistance under constant temperature and pure nitrogen flow (value taken once, before any H<sub>2</sub> exposure), and R is the value of the sensor electrical resistance under H<sub>2</sub> exposure. The response and recovery time presented below are respectively defined as the time needed to reach 90% of the maximal R<sub>s</sub> value for a given H<sub>2</sub> exposure (T<sub>90</sub>) and as the time needed to return from stable R<sub>s</sub> value to 10% of the stable baseline when hydrogen gas was stopped (T<sub>10</sub>).

$$R_s (\%) = [(R - R_0)/R_0] \times 100 \quad (1)$$

### III. PHYSICOCHEMICAL AND ELECTRICAL CHARACTERIZATION

#### A. Chemical composition

Scanning Electron Microscopy (SEM) analysis was performed with a Zeiss Gemini SEM 500 ultra-high resolution Field Emission Scanning Electron Microscope (FESEM). For chemical analyses (Energy Dispersive X-ray Spectroscopy (EDS)), an Energy Dispersive Analysis of X-rays (EDAX) Octane Silicon Drift Detector (129 eV energy resolution for Manganese) was used at 15 kV, with a magnification of 10k on 3μm x 3μm area. Fig. 2 shows X-ray line spectra performed on sample A, with detected elements such as Palladium (Pd), Gold (Au), Silicon (Si) and Carbon (C). Four measurements were performed revealing an estimated alloy composition of 80% Pd and 20% Au.

Visual surface sample inspection is shown in Fig. 3, using SEM 100k magnification. No major variation is observed for surface morphology after annealing. Surface is composed of zones with small grains and zones of merged grains.

#### B. X Ray diffraction

The sample A microstructure was examined by X-ray diffraction, prior and after annealing was performed. The diagrams have been carried out with a theta-theta configuration and CuKα radiation (λ=0.154 nm) using an Empyrean diffractometer, equipped with a rapid detector,

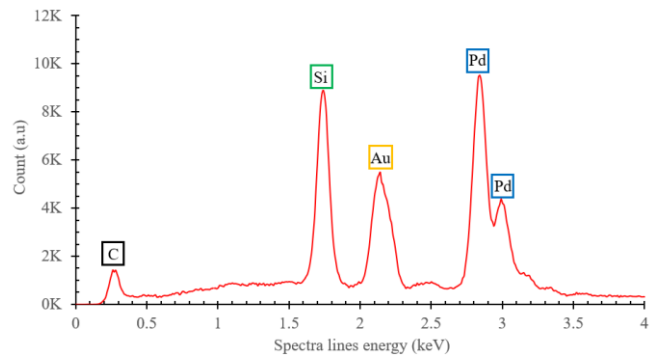


Figure 2. EDX analysis performed on sample A, for ease of reading, Au peak at 9.72 keV is not displayed.

using a 2° offset to avoid to be aligned with Si substrate. The average crystallite grain size (G<sub>s</sub>) was estimated using the Scherrer formula (2).

$$G_s = [0.89 \times \lambda] / [\beta \times \cos\theta] \quad (2)$$

Where λ is the X-ray wavelength, β the FWHM of (111) peak and θ the diffraction angle. Fig. 4 evidences that, for our sputtering parameters and film thickness, the film crystallizes mainly with a (111) preferred orientation and this trend is kept even after annealing. Small diffraction peaks are detected for the (311) and (222) planes; \* symbol refers to SiO<sub>2</sub>/Si substrate diffraction peak. Heat treatment has a noticeable impact on the microstructure with an increase of the crystallinity as (111) peak intensity grows from 13700 to almost 19400 counts. But, as suggested by Fig. 3, the grain size estimated from the Scherrer formula seems to be stable about 20 ±1 nm. Otherwise, the 2θ angle shift of the diffraction peaks is suggesting stress relaxation during the heat treatment.

#### C. Temperature influence on sensor response to hydrogen

Temperature of measurement is of crucial importance as it both affects sensor performance in term of response/recovery time and sensitivity. Furthermore, for practical applications, high operating temperatures are power consuming and hazardous for explosive environment [23]. Response/recovery time is usually reported to decrease with increasing temperature of measurement. Regarding sensor response to H<sub>2</sub> exposure, data vary. Some authors see their response dropping [24] [25], others increasing [20] [25] [26].

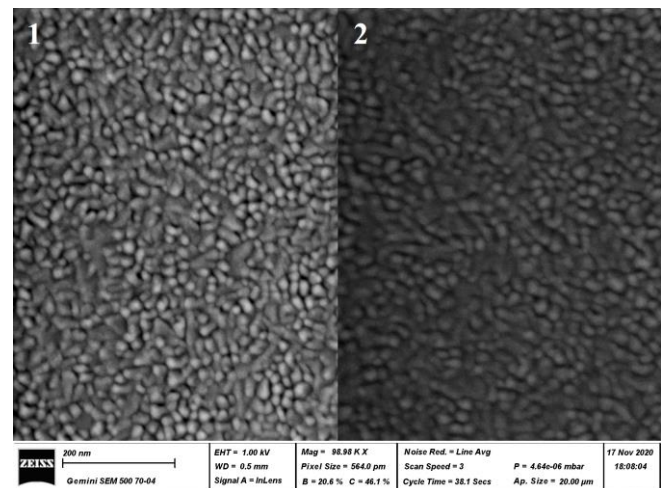


Figure 3. SEM photo of the surface aspect of sample A, before (1) and after annealing (2).

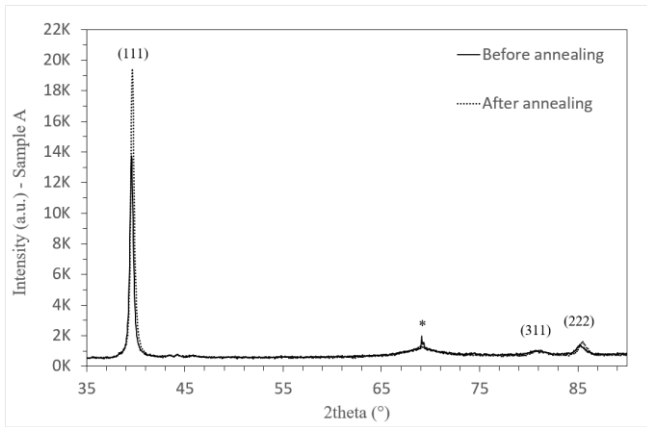


Figure 4. XRD diagram of sample A before and after annealing ( $\lambda=0.154$  nm). The star indicates the trace of the Si substrate diffraction peak.

Fig. 5 shows the sensor response to 0.3% H<sub>2</sub> in N<sub>2</sub> exposure, at various temperatures. Response and recovery time as well as response amplitude are decreasing with increasing temperature. The response (T<sub>90</sub>) and recovery time (T<sub>10</sub>) are respectively 6min50s and 68min at 25°C, 5min40s and 17min30s at 100°C. Those results are in line with previous literature. Regarding sensor amplitude, it can be seen that upon heating, the maximal response value to 0.3% H<sub>2</sub> exposure diminishes and signal tends to become noisy, thus sensor will be less sensitive to H<sub>2</sub> variations. Yet, sensor was found to be operative for hydrogen detection in an anaerobic environment at all temperatures, 1.9% being the maximal response, obtained at 25°C and 0.5% being the lowest response, obtained at 100°C. Best operative temperature was found to be 50°C as it combines sufficient short response and recovery time (6min20s and 21min40s respectively), good sensitivity with 1.3% response toward 0.3% H<sub>2</sub> and a clear signal. Response and recovery time as well as sensor response are plotted for all temperatures in Fig. 6 and Fig. 7 respectively.

The sensor response dropping with increasing temperature can be explained as follows. The hydrogen absorption capacity of Pd and its alloys is linked to their Fermi level and the number of free d-states at this level [27] [28]. When increasing temperature, the number of low energy free d-sites tends to diminish as Fermi level rises, thus, more and more energy is needed for octahedral site occupation. For a given H<sub>2</sub> concentration, less site occupation will occur at elevated temperature, resulting in a lower response amplitude.

Finally, sensor sensitivity to others H<sub>2</sub> concentrations was investigated with a 1.5% and 3% H<sub>2</sub> exposure, results are

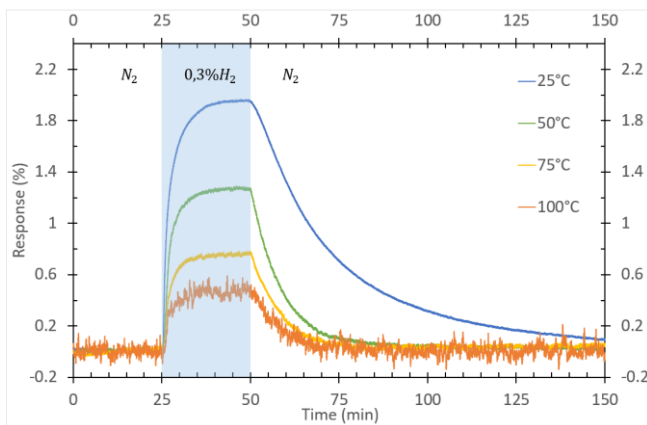


Figure 5. Sensor responses to 0.3% H<sub>2</sub> in N<sub>2</sub> at various temperatures

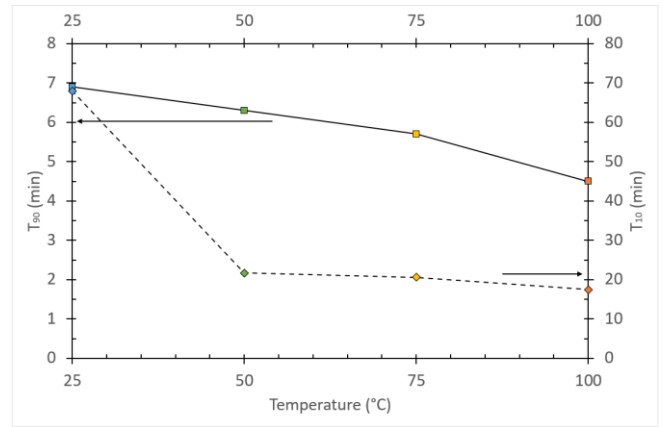


Figure 6. Plot of response (T<sub>90</sub>) and recovery (T<sub>10</sub>) time of sensor for 0.3% H<sub>2</sub> in N<sub>2</sub> at various temperatures.

presented in Fig. 8. Response amplitude is 2.6% for 1.5% H<sub>2</sub> and 3.4% for 3% H<sub>2</sub>. Response and recovery time are respectively 6min20s and 20min20s for 1.5% H<sub>2</sub>, 6min and 20min40s for 3% H<sub>2</sub>. Those data show that our sensor was able to detect hydrogen from low to high concentration with a stable baseline.

Regarding response time, literature usually shows response/recovery time in the order of a few tens of seconds for the same material. An explanation for such difference with our minutes order response time could be due to : (1) thickness and width of our sensor design, simulation [29] show that expanding sensor volume largely increases reaction time; (2) low gas flow compare to cell volume. Fick's second law is usually used to ascribe the hydrogen diffusion dependence to H<sub>2</sub> partial pressure [29]. Thus, a long filling time results in a non-maximal kinetic of diffusion in the sensing layer. Recent work put in evidence long filling time of our cross chamber [30], validating above hypothesis.

#### IV. CONCLUSION AND FURTHER WORK

In summary, we have fabricated a resistive hydrogen sensor, using Pd<sub>0.8</sub>Au<sub>0.2</sub> alloy as sensitive film, by magnetron sputtering and tested it in an anaerobic environment at different temperatures. DRX analysis shows the preferential growth along the (111) plane. Thermal treatment increased the film crystallinity, while grain size remains at 20 ± 1 nm. The best operating temperature was found to be at 50°C as it combines a relative fast response and recovery time, a sufficient response amplitude to 0.3% H<sub>2</sub> in N<sub>2</sub> and a clear and exploitable signal. Sensor was also able to detect hydrogen from low (0.3%) to high concentration (3%). After this preliminary work showing PdAu alloy ability to measure hydrogen in an anaerobic atmosphere, the next steps of the study will concern :

- Characterisation of the sensitivity and selectivity
- Improving response and recovery times
- Testing the effect of different Au contents in the alloy under anaerobic atmospheres containing up to 3%H<sub>2</sub>.

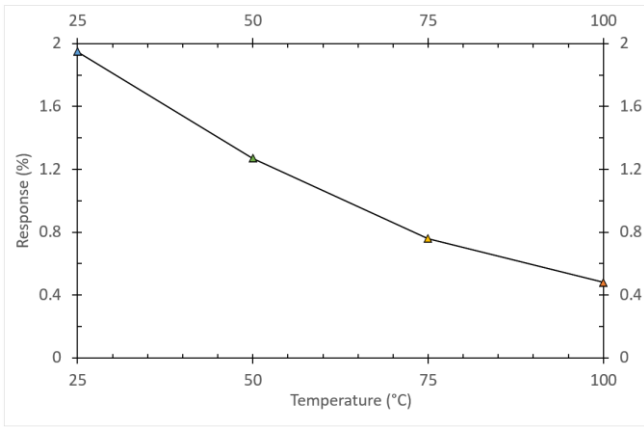


Figure 7. Plot of sensor response for 0.3% H<sub>2</sub> in N<sub>2</sub> at various temperatures.

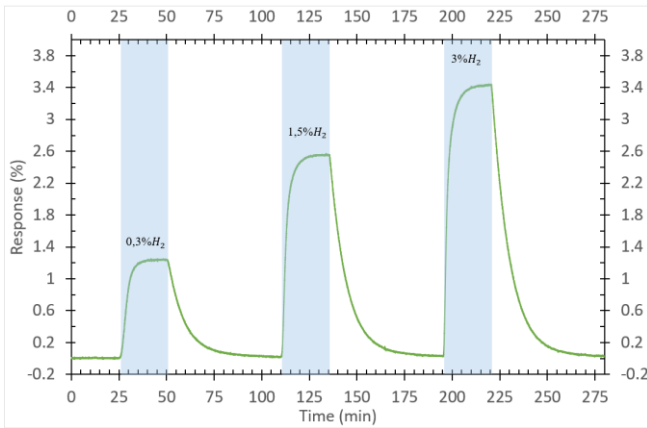


Figure 8. Sensor responses to 0.3%, 1.5% and 3% H<sub>2</sub> in N<sub>2</sub> at 50°C.

#### ACKNOWLEDGMENT

The authors thank Soilihi Moindjie, Jean-Jacques Furter, CP2M laboratory for their technical support and Khaoula El Ouazzani for performing XRD. Clément Occelli would like to thank Région Sud of France and CMR Group for financial support.

## References

- [1] A. Demirbas, 'Future hydrogen economy and policy', *Energy Sources, Part B: Economics, Planning, and Policy*, vol. 12, no. 2, pp. 172–181, Feb. 2017, doi: 10.1080/15567249.2014.950394.
- [2] Z. Abdin et al., 'Hydrogen as an energy vector', *Renewable and Sustainable Energy Reviews*, vol. 120, p. 109620, Mar. 2020, doi: 10.1016/j.rser.2019.109620.
- [3] C. Acar and I. Dincer, 'Review and evaluation of hydrogen production options for better environment', *Journal of Cleaner Production*, vol. 218, pp. 835–849, May 2019, doi: 10.1016/j.jclepro.2019.02.046.
- [4] D. Haeseldonckx and W. D'haeseleer, 'The use of the natural-gas pipeline infrastructure for hydrogen transport in a changing market structure', *International Journal of Hydrogen Energy*, vol. 32, no. 10, pp. 1381–1386, Jul. 2007, doi: 10.1016/j.ijhydene.2006.10.018.
- [5] A. Maroufmashat and M. Fowler, 'Transition of Future Energy System Infrastructure; through Power-to-Gas Pathways', *Energies*, vol. 10, no. 8, p. 1089, Jul. 2017, doi: 10.3390/en10081089.
- [6] M. Kong et al., 'Investigation of Mixing Behavior of Hydrogen Blended to Natural Gas in Gas Network', *Sustainability*, vol. 13, no. 8, p. 4255, Apr. 2021, doi: 10.3390/su13084255.
- [7] A. S. Ruhl and A. Kranzmann, 'Investigation of corrosive effects of sulphur dioxide, oxygen and water vapour on pipeline steels', *International Journal of Greenhouse Gas Control*, vol. 13, pp. 9–16, Mar. 2013, doi: 10.1016/j.ijggc.2012.12.007.
- [8] S. Younus Ahmed, P. Gandhidasan, and A. A. Al-Farayedhi, 'Pipeline drying using dehumidified air with low dew point temperature', *Applied Thermal Engineering*, vol. 18, no. 5, pp. 231–244, Jan. 1998, doi: 10.1016/S1359-4311(97)00083-5.
- [9] Y. Luo, C. Zhang, B. Zheng, X. Geng, and M. Debliquy, 'Hydrogen sensors based on noble metal doped metal-oxide semiconductor: A review', *International Journal of Hydrogen Energy*, vol. 42, no. 31, pp. 20386–20397, Aug. 2017, doi: 10.1016/j.ijhydene.2017.06.066.
- [10] W.-T. Koo et al., 'Chemiresistive Hydrogen Sensors: Fundamentals, Recent Advances, and Challenges', *ACS Nano*, vol. 14, no. 11, pp. 14284–14322, Nov. 2020, doi: 10.1021/acsnano.0c05307.
- [11] T. Hübert, L. Boon-Brett, G. Black, and U. Banach, 'Hydrogen sensors – A review', *Sensors and Actuators B: Chemical*, vol. 157, no. 2, pp. 329–352, Oct. 2011, doi: 10.1016/j.snb.2011.04.070.
- [12] W. J. Buttner et al., 'Inter-laboratory assessment of hydrogen safety sensors performance under anaerobic conditions', *International Journal of Hydrogen Energy*, vol. 37, no. 22, pp. 17540–17548, Nov. 2012, doi: 10.1016/j.ijhydene.2012.03.165.
- [13] Y. Du et al., 'Aerobic and anaerobic H<sub>2</sub> sensing sensors fabricated by diffusion membranes depositing on Pt-ZnO film', *Sensors and Actuators B: Chemical*, vol. 252, pp. 239–250, Nov. 2017, doi: 10.1016/j.snb.2017.06.005.
- [14] A. Mirzaei et al., 'An overview on how Pd on resistive-based nanomaterial gas sensors can enhance response toward hydrogen gas', *International Journal of Hydrogen Energy*, p. S0360319919320944, Jun. 2019, doi: 10.1016/j.ijhydene.2019.05.180.
- [15] C. Wadell et al., and C. Langhammer, 'Hysteresis-Free Nanoplasmonic Pd–Au Alloy Hydrogen Sensors', *Nano Lett.*, vol. 15, no. 5, pp. 3563–3570, May 2015, doi: 10.1021/acs.nanolett.5b01053.
- [16] S. Luo, D. Wang, and T. B. Flanagan, 'Thermodynamics of Hydrogen in fcc Pd–Au Alloys', *J. Phys. Chem. B*, vol. 114, no. 18, pp. 6117–6125, May 2010, doi: 10.1021/jp100858r.
- [17] Z. Zhao, M. A. Carpenter, H. Xia, and D. Welch, 'All-optical hydrogen sensor based on a high alloy content palladium thin film', *Sensors and Actuators B: Chemical*, vol. 113, no. 1, pp. 532–538, Jan. 2006, doi: 10.1016/j.snb.2005.03.070.
- [18] R. J. Westerwaal et al., 'Nanostructured Pd–Au based fiber optic sensors for probing hydrogen concentrations in gas mixtures', *International Journal of Hydrogen Energy*, vol. 38, no. 10, pp. 4201–4212, Apr. 2013, doi: 10.1016/j.ijhydene.2012.12.146.
- [19] L. J. Bannenberg et al., 'Direct Comparison of PdAu Alloy Thin Films and Nanoparticles upon Hydrogen Exposure', *ACS Appl. Mater. Interfaces*, vol. 11, no. 17, pp. 15489–15497, May 2019, doi: 10.1021/acsmi.8b22455.
- [20] Q. Liu, J. Yao, Y. Wang, Y. Sun, and G. Ding, 'Temperature dependent response/recovery characteristics of Pd/Ni thin film based hydrogen sensor', *Sensors and Actuators B: Chemical*, vol. 290, pp. 544–550, Jul. 2019, doi: 10.1016/j.snb.2019.04.024.
- [21] M. W. Jenkins, R. C. Hughes, and S. V. Patel, 'Stabilizing the response of Pd/Ni alloy films to hydrogen with Ti adhesion layers', Boston, MA, Feb. 2001, p. 99. doi: 10.1117/12.417437.
- [22] Z. Zhao and M. A. Carpenter, 'Annealing enhanced hydrogen absorption in nanocrystalline Pd/Au sensing films', *Journal of Applied Physics*, vol. 97, no. 12, p. 124301, Jun. 2005, doi: 10.1063/1.1927690.
- [23] I. Darmadi, F. A. A. Nugroho, and C. Langhammer, 'High-Performance Nanostructured Palladium-Based Hydrogen Sensors—Current Limitations and Strategies for Their Mitigation', *ACS Sens.*, p. acssensors.0c02019, Nov. 2020, doi: 10.1021/acssensors.0c02019.
- [24] M. Wang and Y. Feng, 'Palladium–silver thin film for hydrogen sensing', *Sensors and Actuators B: Chemical*, vol. 123, no. 1, pp. 101–106, Apr. 2007, doi: 10.1016/j.snb.2006.07.030.
- [25] K. Yu et al., 'Enhanced accuracy of palladium-nickel alloy based hydrogen sensor by in situ temperature compensation', *Sensors and Actuators B: Chemical*, vol. 299, p. 126989, Nov. 2019, doi: 10.1016/j.snb.2019.126989.
- [26] B. Sharma and J.-S. Kim, 'Pd/Ag alloy as an application for hydrogen sensing', *International Journal of Hydrogen Energy*, vol. 42, no. 40, pp. 25446–25452, Oct. 2017, doi: 10.1016/j.ijhydene.2017.08.142.
- [27] M. Hara et al., 'Evaluation of terminal composition of palladium–silver hydrides in plateau region by electronic structure calculations', *Journal of Alloys and Compounds*, vol. 580, pp. S202–S206, Dec. 2013, doi: 10.1016/j.jallcom.2013.03.095.
- [28] S. Akamaru, M. Hara, N. Nunomura, and M. Matsuyama, 'Effect of substituting elements on hydrogen uptake for Pd–Rh–H and Pd–Ag–H systems evaluated by magnetic susceptibility measurement', *International Journal of Hydrogen Energy*, vol. 38, no. 18, pp. 7569–7575, Jun. 2013, doi: sakamoto.
- [29] Y. Liu, Y. Li, P. Huang, H. Song, and G. Zhang, 'Modeling of hydrogen atom diffusion and response behavior of hydrogen sensors in Pd–Y alloy nanofilm', *Scientific Reports*, vol. 6, no. 1, pp. 1–9, Nov. 2016, doi: 10.1038/srep37043.
- [30] F.-E. Annanouch et al., 'Hydrodynamic evaluation of gas testing chamber: Simulation, experiment', *Sensors and Actuators B: Chemical*, vol. 290, pp. 598–606, Jul. 2019, doi: 10.1016/j.snb.2019.04.023.